Studying of nanocomposite films' structure and properties obtained by magnetron sputtering

2016 IOP Conf. Ser.: Mater. Sci. Eng. 110 012004

(http://iopscience.iop.org/1757-899X/110/1/012004)

Studying of nanocomposite films' structure and properties obtained by magnetron sputtering

Y O Tleukenov[1], S V Plotnikov[1], N K Erdybaeva[1], A D Pogrebnyak[2]

[1] *Ust-Kamenogorsk, 070003, Kazakhstan,* D. Serikbayev East Kazakhstan State Technical University, 23/2-54 Serikbayev Street
[2] *Sumy, 40000, Ukraine,* Sumy State University, Rimsky-Korsakov Street, 2

E-mail: erick_090@mail.ru

Abstract.

Various approaches to creating multicomponent na-nocomposite coatings of high and superhigh hardness (from 30 to 100 ± 120 GPa) are reviewed with particular emphasis placed on mechanisms underlying the increase in hardness in thin coatings. Nanocomposite Nb-Al-N films fabricated by magnetron sputtering were researched in this work. Two stable crystalline structural states were found in the films: NbN_{ch} and solid solution B1-$Nb_xAl_{1-x}N_yO_{1-y}$, and also an amorphous component associated with aluminum oxynitride with reactive magnetron sputtering. A relationship of substructural characteristics sensitivity with the current and nanohardness and Knoop hardness characteristic was determined in this paper. Recent changes in the range of 29-33.5 GPa and 46-48 GPa, respectively. Initial principle calculations of NbN and Nb_2AlN phases and NbN/AlN heterostructures were carried out for the interpretation of the results. Deposited nanocomposite films with the given mechanical properties may be used as wear resistant or protective coatings. On the basis of these results, it can be assumed that two stable crystalline structural states were found in the films: B1-NbN_x and solid solution with a composition close to the B1-$Nb_{0.67}Al_{0.33}N$. The films also contain an amorphous component associated with aluminum nitride.

1. Introduction

Creation of new materials, including multicomponent nano-composite coatings with a characteristic grain size below 100 nm, is a priority area of modern science and technology. Nanotechnologies are expected to become the principal driving force in scientific and technical developments by the mid-21st century. Nanothechnology is a field focusing on the control of matter on the atomic, molecular, and supramole-cular scales (in a range of sizes from 1 to 50 nm) for the creation, processing, and application of materials, devices, and systems having novel properties and functional capabil-ities due to the small size of their structural elements. Nanomaterials may be classified by the size and geometric shape of their structural elements. The main types of nanomaterials in terms of grain size are cluster and fiber materials, films and coatings, multilayer (multi-component) structures, and bulk nanocrystalline materials whose grains have nanometer dimensions in all three directions. Nanocomposite coatings exemplify materials of a new generation, composed of at least two phases with a nanocrys-talline and/or amorphous structure. Because of the very small size (4 10 nm) of their

grains and more important role of boundary zones surrounding single grains, nanocomposite materials behave unlike traditional materials with a grain size over 100 nm and display quite different properties. The novel unique physical and functional properties of nanocomposites constitute a driving force for the rapid development of nanocomposite materials [20 ± 30]. Films with the hardness H 4 40 GPa and H > 40 GPa are currently described as hard and superhard, respectively.

Films based on NbN and (Ti-Zr-Hf-V)N show many interesting properties such as high hardness and electrical conductivity, thermal stability and chemical inertness [1]. NbN and (Ti-Zr-Hf-V)N films are used as the cathode material for field electron emission in vacuum of microelectronic devices [2]. It was shown that the introduction of Al atoms into the lattice led to the formation of solid solution $Nb_{1-x}Al_xN$. For solid solutions $Nb_{1-x}Al_xN$, B1 (type - NaCl) structure is more preferable for x below 0.45. In the range of x = 0.45-0.71, the mixture of structures B1 and B4 was observed, while when x> 0.71, B4 structure (type - wurtzite with a hexagonal structure) was formed [6,7]. Films Nb-Al-N composed of solid solution $Nb_{1-x}Al_xN$ with B1 (rare B_K) and B4 structures or mixtures thereof [3-7]. On the other hand, hitherto, nanocomposite NbN/AlN films were not investigated. Thus, in the present study, we set out to research the Nb-Al-N film and multi-element (Ti-Zr-Hf-V)N coatings, arguing that under certain conditions can be formed nanocomposite structure of the films, which may have improved mechanical properties.

2. Experimental details

Nb-Al-N and (Ti-Zr-Hf-V)N coatings deposited on the mirror-polished wafer Si (100) using a DC magnetron sputtering Nb (99.9%, Ø72 x 4 mm) and Al (99.999%, Ø72 x 4 mm) under argon and nitrogen with the following parameters of deposition: the substrate temperature T_S = 350°C; substrate bias voltage U_B = -50 V; The flow rate (F) F_{Ar} = 40 sccm; F_{N2} = 13 sccm; operating pressure P_C = 0.17 Pa. The current supplied to the target Al (I_{Al}) was 100, 150, 200, 250 and 300 mA, which corresponds to the discharge power density P_{Al} = 5.7, 8.6, 11.4, 13.7 and 17.1 W/cm^2, respectively. Current supplied to the target Nb (I_{Nb}) was 300 mA (P_{Nb} = 17.1 W/cm^2). The base pressure in the vacuum chamber was better than 10^{-4} Pa. The distance between the target and the substrate holder was 8 cm. The dihedral angle between the targets was ~ 45^0. Substrates were ultrasonically cleaned before they were placed in a vacuum chamber. Furthermore, prior to deposition, the substrates were etched in a vacuum chamber in the hydrogen plasma for 5 min.

3. Results and discussion

Structural and mechanical properties were analyzed depending on I_{Al}.values. The structure of the coatings was researched by X-ray diffraction (XRD, diffractometer DRON-3M) in CuK_α radiation. The program of authoring profiles sharing was used with the application of complex diffraction profiles. Substructural characteristics (crystallite and microstrain size) were determined by approximation using the approximation function as - Cauchy function. The spectrum of Fourier spectroscopy (FTIR) was measured at room temperature in the range of 400−4000 cm^{-1} by spectrometer "TSM 1202" LTD «Infraspek». Knoop hardness (HK) was assessed using microhardnessmeter Microhardness Tester Micromet 2103 BUEHLER LTD under a load of 100 mN, and by nanoindentation using nanohardnessmeter G-200, equipped with a Berkovich indenter. The loads were chosen in such conditions that the indenter penetration wouldn't exceed 10-20% of the film hickness. The film thickness was determined by optical profilometer "Micron-gamma". The thickness values of the Nb-Al-N coatings depends weakly on I_{Al}. D and were in the range of 0.7-0.9 μm, for (Ti-Zr-Hf-V)N the thickness values were in the range of 30-90 μm.

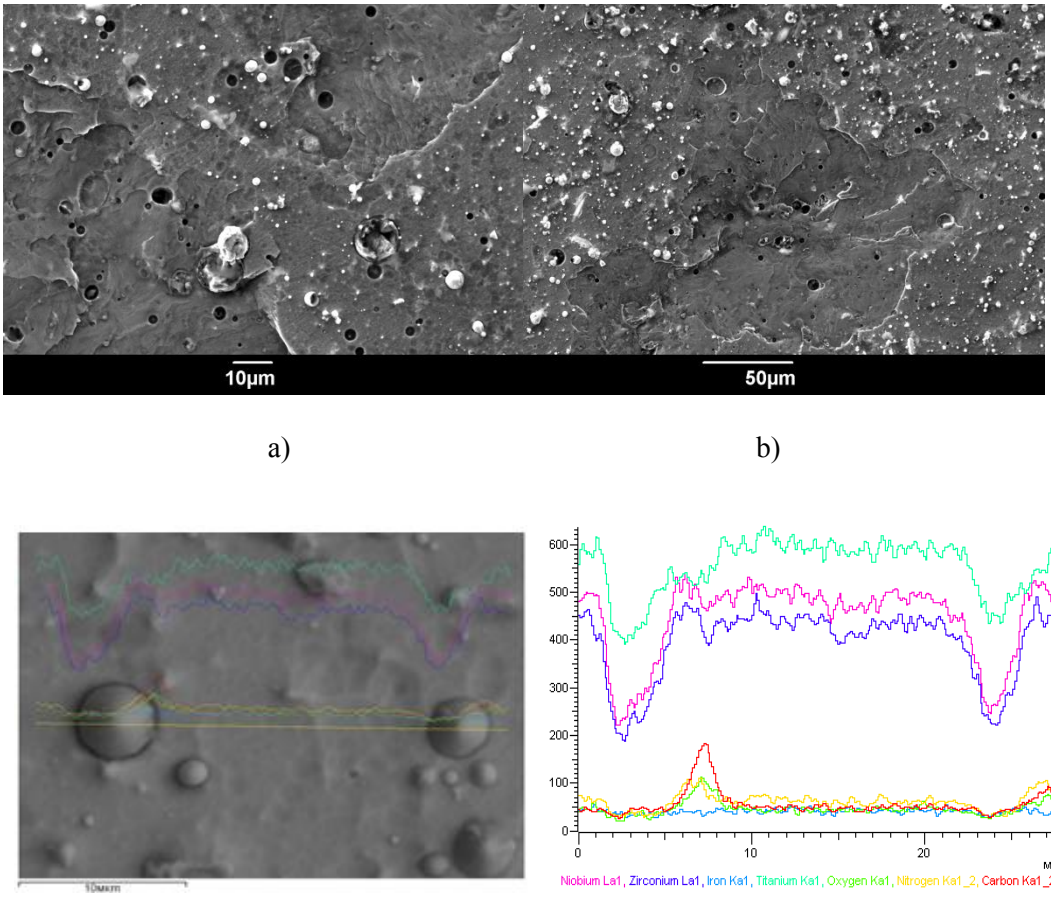

Figure 1. SEM images showing the surface (a-c) of (Ti-Zr-Hf-V)N coatings and elements contribution deposited by magnetron sputtering.

Figure 1 shows as an example the composition morphology of (Ti-Zr-Hf-V)N coatings deposited by reactive magnetron sputtering under applied steel 45 substrate. Where, the coatings deposited under magnetron sputtering show low concentrations of oxygen which originated from the water absorbed during exposure of the coatings to air after their deposition. These examples confirm that care must be taken when depositing hard and superhard coatings for application on tools. Elements concentration is shown in the table 1.

Table 1. Elemental analysis, in%.

Spectrum	O	Ti	V	Zr	Hf	Au	Hg	Total
Total spectrum	8.86	19.03	6.05	12.54	34.10	12.16	7.27	100.00
Average	8.86	19.03	6.05	12.54	34.10	12.16	7.27	100.00
Std. deviation	0.00	0.00	0.00	0.00	0.00	0.00	0.00	
Max	8.86	19.03	6.05	12.54	34.10	12.16	7.27	
Min	8.86	19.03	6.05	12.54	34.10	12.16	7.27	

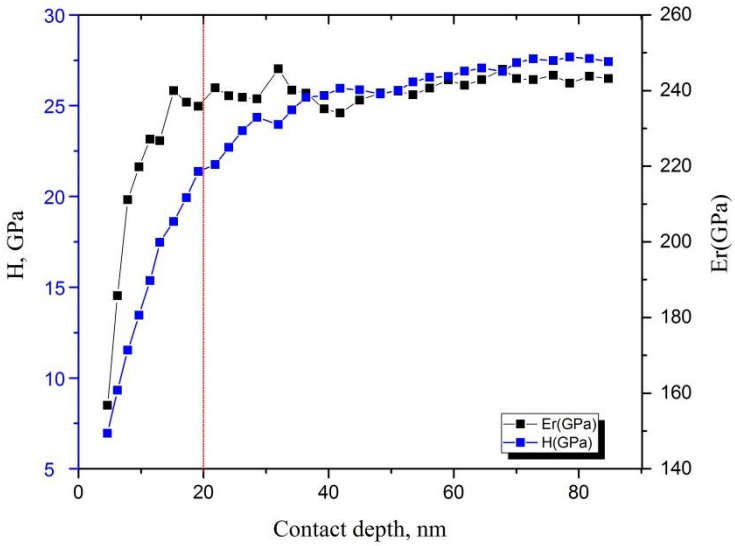

Figure 2. The results of the mechanical studies of (Ti-Zr-Hf-V)N coatings.

Figure 2 shows the results of dynamic indentation pyramid Berkovich (triboindentor). We can estimate the depth of the indentation to determine the value of the reduced modulus of elasticity. The measurements were made when the load on the indenter 500 10 000 μN (Ti-Zr-Hf-V)N coatings. The corresponding dependence of nanohardness and reduced modulus of elasticity Er on the penetration depth for the mode was also shown. Nanohardness increased to almost 27 GPa where the layer thickness was 30 nm with gradual access to the horizontal line to the penetration depth of 85 nm.

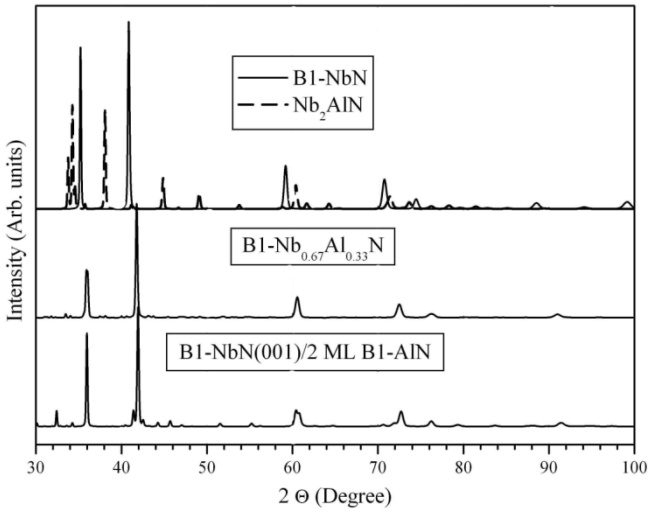

Figure 6. The calculated X-ray diffraction patterns.

Using atomic configurations resulting from first-principles calculations, we calculated diffraction patterns for the B1−$NbN_ц$, B1−$Nb_xAl_{1-x}N$, x ~ 0.67 и Nb_2AlN. The calculated XRD spectra are shown in Figure 4. Comparison of the calculated and experimental spectra (Figure 6) shows that reflexes about $2\Theta \sim 32^0$ associated with the heterostructure, and about $2\Theta \sim 38^0$, resulted by phase Nb_2AlN and does not occur at the experimental spectra. Therefore, we can assume that our films contain neither

Nb_2AlN, nor any epitaxial layers B1-AlN, but rather consist of crystallites B1−NbN_{ch} and B1−$Nb_xAl_{1-x}N$, $x \sim 0.67$. As the matter of fact, the difference between the peak positions $\Delta 2\Theta = 2\Theta\cdot(B1-NbN_{ч})-2\Theta\cdot(B1-Nb_xAl_{1-x}N)$ for each diffraction peak (200) and (400) on experimental and theoretical diffraction patterns is almost identical. We should also note that films of niobium nitride are prone to accumulate small amounts of oxygen [5]. Oxygen can replace part of the nitrogen in solid solution and in the amorphous matrix [8-17]. Therefore, structure $Nb_xAl_{1-x}N_yO_{1-y}$, x~0.67, 1-y << 1will be more realistic for the solid solutions, as for the amorphous matrix - a-AlNO, which was shown as a result of elemental analysis, obtained by SIMS, RBS and EDS in these films.

4. Conclusion

Films Nb-Al-N were deposited on silicon substrates by magnetron sputtering targets of Nb and Al at different discharge powers at the target of aluminum. Experimental and theoretical studies show that the films obtained at selected deposition parameters have the nanocomposite structure that represents the nanocrystals B1−NbN_x and B1-$Nb_xAl_{1-x}N_yO_{1-y}$, embedded in a-AlNO matrix (nc−B1−NbN_x/nc−B1−$Nb_xAl_{1-x}N_eO_{1-y}$/a−AlNO). Nanocomposite coating with high microstrain action due to the difference in atomic radius of the crystal lattices metal components shows high hardness values (up to 32 GPa). Deposited nanocomposite films may be recommended with the given mechanical properties as wear resistant or protective coatings.

References

[1] Barnett S A, Madan A, Kom I, Martin K 2003 *Mrs Bulletin*. 28, pp. 169.
[2] Gotoh Y, Nagao M, Ura T, Tsuji H, Ishikawa J 1999 *Nucl. Instr. Methods Phys. Res.* Vol. **148** pp. 925.
[3] Selinder T I, Miller D J, Gray K E 1995 *Vacuu* vol. **46** pp. 1401.
[4] Makino Y, Saito K, Murakami Y, Asami K 2007 *Solid State phenomena* vol. **127** pp. 195.
[5] Barshilla H C, Deepthi B, Rajam K S. Mater J 2008 *Res.* Vol. **23** pp. 1258.
[6] Franz R, Lechthaler M, Polzer C, Mitterer C 2010 *Surf. Coat. Technol.* Vol. **204**, 2447.
[7] Holec D, Franz R, Mayrhofer P H, Mitterer C 2010 *J. Phys.* Vol. **41**, 145403.
[8] X-ray powder diffraction file [038-1155].
[9] Umanski Y S, Skakov Y A 1978 Physica metallov. Atomnoe stroenie metallov i splavov *Atomizdat M.* pp. 352.
[10] Jadannadham K, Sharma A K, Wei Q, Kalyanraman R, Narayan 1998 *Vac. Sci. Technol* vol. **16**, 2804.
[11] Ivashchenko V I, Veprek S, Scrynskyy P L, Lytvyn O, Butenko O O, Sinelnichenko O K, Gorb L, Hill F, Leszczynski J, Kozak A O 2014 *Superhard Materials* vol. **36**, pp. 1.
[12] Ivashchenko V I, Veprek S, Turchi P E A, Shevchenko V I 2012 *Phys. Rev.* Vol. **85,** 195403-1.
[13] Giannozzi P, Baroni S, Bonini N, Calandra M, Car R, Cavazzoni C, Ceresoli D, Chiarotti G L, CococcioniI M. Dabo, Dal Corso A, de Gironcoli S, Fabris S, Fratesi G, Gebauer R, Gerstmann U, Gougoussis C, Kokalj A, Lazzeri M, Martin-Samos L, Marzari N, Mauri F, Mazzarello R, Paolini S, Pasquarello A, Paulatto L, Sbraccia C, Scandolo S, Sclauzero G, Seitsonen A P, Smogunov A, Umari P, Wentzcovitch R M 2009 *Phys.: Cond. Matter* vol. **21,** 395502-19.
[14] Perdew J P, Burke K, Ernzerhof M 1996 *Phys. Rev. Lett.* **77,** 3865.
[15] Kraus W, Nolze G 2000 PowderCell for Windows, version 2.4.
[16] Ivashchenko V, Veprek S, Pogrebnjak A,Postolnyi B 2014 *Sci. Tech. Adv. Mater*. Vol **15,** 025007-11.
[17] Pogrebnjak A D, Bagdasaryan A A, Yakushchenko I V, Beresnev V M 2014 *Rus. Chem. Rev.* Vol **83**, 1027.